ACS APPLIED MATERIALS & INTERFACES

Research Article

www.acsami.org

Core–Shell Fe_3O_4 Polydopamine Nanoparticles Serve Multipurpose as Drug Carrier, Catalyst Support and Carbon Adsorbent

Rui Liu,[†] Yunlong Guo,[†] Gloria Odusote,[†] Fengli Qu,[†,‡] and Rodney D. Priestley*[,†,§]

[†]Department of Chemical and Biological Engineering and [§]Princeton Institute for the Science and Technology of Materials, Princeton University, Princeton, New Jersey 08544, United States

[‡]College of Chemistry and Chemical Engineering, Qufu Normal University, Qufu 273165, China

Supporting Information

ABSTRACT: We present the synthesis and multifunctional utilization of core–shell Fe_3O_4 polydopamine nanoparticles (Fe_3O_4@PDA NPs) to serve as the enabling platform for a range of applications including responsive drug delivery, recyclable catalyst support, and adsorbent. Magnetite Fe_3O_4 NPs formed in a one-pot process by the hydrothermal approach were coated with a polydopamine shell layer of ~20 nm in thickness. The as prepared Fe_3O_4@PDA NPs were used for the controlled drug release in a pH-sensitive manner via reversible bonding between catechol and boronic acid groups of PDA and the anticancer drug bortezomib (BTZ), respectively. The facile deposition of Au NPs atop Fe_3O_4@PDA NPs was achieved by utilizing PDA as both the reducing agent and the coupling agent. The nanocatalysts exhibited high catalytic performance for the reduction of *o*-nitrophenol. Furthermore, the recovery and reuse of the catalyst was demonstrated 10 times without any detectible loss in activity. Finally, the PDA layers were converted into carbon to obtain Fe_3O_4@C and used as an adsorbent for the removal of Rhodamine B from an aqueous solution. The synergistic combination of unique features of PDA and magnetic nanoparticles establishes these core–shell NPs as a versatile platform for multiple applications.

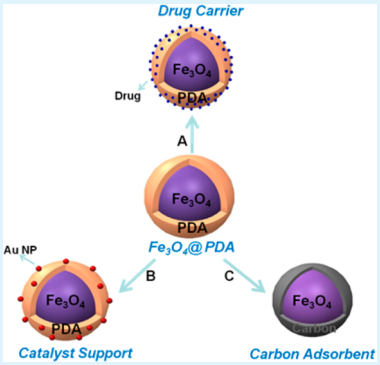

KEYWORDS: *core-shell nanoparticles, polydopamine, dopamine, Fe_3O_4, multi-functional*

1. INTRODUCTION

Uniform core–shell nanoparticles with magnetically responsive cores and functional shells are being widely investigated because of their potential applications in cell separation, enzyme immobilization, protein and nucleic acid purification, targeted drug delivery, environmental remediation separation, catalysis, and magnetic resonance imaging.[1−3] There have been extensive reports on the synthesis of magnetic Fe_3O_4 core–shell nanoparticles in which the shell layer was composed of either an inorganic (e.g., silica or gold) or an organic (e.g., polymer) material. In the case of polymer shell layers, polydopamine (PDA) has received significant attention as a candidate material because of its unique coating quality and functionality.[4,5] Dopamine, the PDA monomer that contains both catechol and amine functional groups, self-polymerizes at alkaline pH values.[4] During polymerization, PDA will spontaneously form a conformal and continuous coating layer atop nearly any material present in the reaction media including noble metals, metal oxides, semiconductors, ceramics, and synthetic polymers via the strong binding affinity of catechol functional groups.[4] The PDA layer thickness may be controlled by varying the dopamine concentration and reaction time.[6]

Polydopamine-coated Fe_3O_4 nanoparticles (Fe_3O_4@PDA) have been exploited for use in numerous advanced applications, including the separation and enrichment of proteins in proteomic analysis,[7] the detection of pollutants by matrix-assisted laser desorption/ionization time-of-flight mass spectrometry,[8] and magnetic solid-phase extraction adsorbent for the determination of trace polycyclic aromatic hydrocarbons in environmental samples.[9] PDA can serve as an adhesion layer to immobilize biological molecules, amine- and mercapto-functionalized self-assembled monolayers, and metal films to the surface for secondary modification as biosensors,[10,11] support for biomineralization[12] and freestanding films,[13] and cancer imaging agents.[14] Fe_3O_4@PDA functionalized with azido groups by reaction with 4-azidobutylamine allowed for the straightforward Cu-catalyzed "click"-reaction with alkynes for the binding of biotin, glucose, proline, or dansyl.[15]

Besides its biocompatibility and adhesiveness, PDA has other attractive material properties. Polydopamine is known to reduce metal salts within a solution into metal nanoparticles via the catechol functional groups.[4,16] A range of metals including Au, Ag, Pt, and Cu have been successfully reduced and deposited atop PDA modified surfaces without the need for the addition of a reducing agent.[4,16] In addition, PDA has been shown to be an effective carbon source for the formation of carbon-coated materials.[17]

Here, we exploit the above-mentioned unique properties of PDA in the formation of Fe_3O_4@PDA core–shell nanoparticles to create a nanostructured metal catalyst support and a

Received: July 1, 2013
Accepted: August 20, 2013
Published: September 6, 2013

Scheme 1. Fe_3O_4@PDA as a Versatile Nanoparticle Platform for (a) Responsive Drug Delivery, (b) Catalyst Support, and (c) Carbon Adsorbent

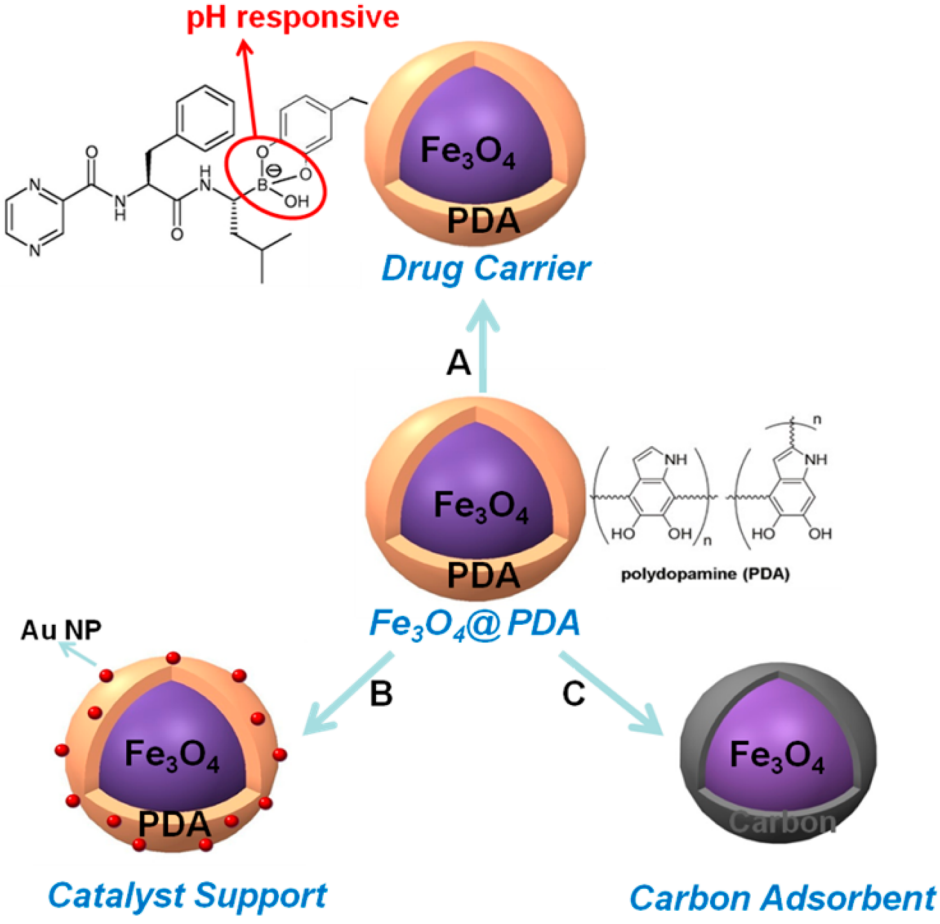

nanostructured adsorbent. Furthermore, we demonstrate that the catechol functional groups on the surface of PDA coated nanoparticles can be exploited to create an environmentally sensitive nanoparticle drug carrier system based on the catechol-boronic acid conjugate pH sensitive reversible bonding.[18,19] Hence, one nanoscale hybrid system, that is, Fe_3O_4@PDA core–shell nanoparticles may be exploited in unique ways for multiple purposes as illustrated in Scheme 1. By taking advantage of the catechol functionality of PDA, Fe_3O_4@PDA can serve as a pH-responsive drug carrier (Scheme 1A). Using PDA as a reducing agent, Fe_3O_4@PDA could be used as a platform to grow and support Au nanoparticles for catalysis (Scheme 1B). Finally, the ability to convert Fe_3O_4@PDA into Fe_3O_4@C (magnetite-carbon core–shell nanoparticles) under heat treatment allows for the formation of a magnetic carbon adsorbent (Scheme 1C). Here, we establish the multi-functional capabilities of Fe_3O_4@PDA core–shell nanoparticles by demonstrating three new advanced applications.

2. EXPERIMENTAL SECTION

Synthesis of Fe_3O_4@PDA. Magnetite Fe_3O_4 nanospheres were prepared by a one-pot hydrothermal method according to a previous report.[20] Typically, 0.325 g of $FeCl_3$ and 0.2 g of trisodium citrate dehydrate were dissolved in 20 mL of ethylene glycol under vigorous stirring for 1 h at room temperature. Subsequently, 1.2 g of sodium acetate was added while stirring for 30 min. The mixture was then sealed in a Teflon-lined stainless-steel autoclave. After reaction for 12 h at 200 °C, the autoclave was cooled to room temperature. The resulting Fe_3O_4 nanoparticles (NPs) were washed with ethanol and ultrapure water three times, respectively, and then dried under vacuum for 12 h. To prepare Fe_3O_4@PDA core–shell nanoparticles, 40 mg of the as-prepared Fe_3O_4 NPs were dispersed in 20 mL of 2 mg/mL dopamine Tris solution (pH 8.5, 10 mM Tris–HCl buffer) and allowed to proceed for 8 h under stirring at room temperature. The resultant product was separated and collected with a magnet and subsequently put through three wash cycles and dried under vacuum overnight.

Synthesis of Au/Fe_3O_4@PDA and Fe_3O_4@C. A 2 mg portion of Fe_3O_4@PDA was well dispersed in a 25 mL chloroauric acid (5μg/mL) aqueous solution. The mixture was stirred at 90 °C for 0.5 h. After the reaction, the resulting Au NPs-deposited Fe_3O_4@PDA were magnetically separated from the suspension, and subsequently washed with ultrapure water 3 times and dried under vacuum overnight. Fe_3O_4@C was obtained by carbonizing Fe_3O_4@PDA under a N_2 atmosphere at 600 °C for 1 h with a heating rate of 1 °C/min using a MTI OTF-1200X tube furnace.

Drug Delivery Test. A 10 mg portion of Fe_3O_4@PDA was stirred in 0.5 mL of a 2 mM dimethyl sulfoxide (DMSO) solution of bortezomib (BTZ) at room temperature for 24 h. The precipitate was magnetically separated and collected, and gently washed with pH 7.0 water. The amount of drug adsorbed was calculated by measuring the difference of supernatant's UV absorbance at 260 nm before and after adsorption. To investigate the pH-responsive properties, drug-loaded particles (2.0 mg) were dispersed in 3 mL of PBS (Phosphate Buffered Saline) buffer at a preselected pH. The release of BTZ was monitored by measuring the UV absorbance at 260 nm as a function of time. UV absorbance was measured at different pHs to construct a standard curve.

Catalytic Study. A 1 mL portion of 0.1 mM *o*-nitrophenol was mixed with a freshly prepared aqueous solution of $NaBH_4$ (2 mL, 0.1M). Au/Fe_3O_4@PDA (1 mg) was then added. UV/Vis absorption spectra were recorded to monitor the change in the reaction mixture after the removal of the nanoparticles. After the reduction process was completed, the catalysts were magnetically separated from the mixture and dried in a vacuum oven overnight for reuse in the next cycle—this process was repeated 10 times.

Adsorption Test. A 5 mg portion of Fe_3O_4@C and 1 mL of aqueous solution of Rhodamine B with various concentrations (0.001−0.012 mg/mL) were mixed and shaken at room temperature for 1 h. The dye loaded Fe_3O_4@C was separated by an external magnet. The concentrations of Rhodamine B remaining in the solutions were determined by measuring the solution UV absorbance at 554 nm. The amount of Rhodamine B adsorbed onto the nanoparticles was calculated using the difference between solution concentrations before and after adsorption.

3. RESULTS AND DISCUSSION

The magnetite nanoparticles Fe_3O_4 were synthesized by a solvothermal reaction at 200 °C by reduction of $FeCl_3$ with ethylene glycol in the presence of sodium acetate, an alkali source, and trisodium citrate, a biocompatible electrostatic stabilizer.[20] Figure 1a illustrates transmission electron microscopy (TEM) image of the magnetite nanoparticles. As revealed in Figure 1a, the NPs are nearly spherical in shape and uniform in size with a diameter of ∼240 nm (hydrodynamic diameter determined by dynamic light scattering (DLS) is provided in Supporting Information, Figure S1). The X-ray diffraction (XRD) patterns of the as-synthesized Fe_3O_4 nanoparticles exhibited the characteristic peaks for magnetite (JCPDS Card no. 19-629, see Supporting Information, Figure S2). Figure 1b presents TEM images of Fe_3O_4@PDA prepared via mixing Fe_3O_4 nanoparticles in a dopamine Tris solution. As illustrated, uniform Fe_3O_4@PDA NPs with a well-defined core−shell structure were successfully synthesized. That is, the Fe_3O_4 NPs, which represent the core, were successfully coated with a thin polydopamine shell layer of ∼20 nm in thickness.

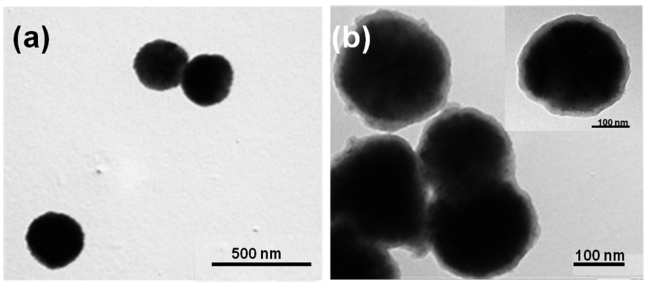

Figure 1. TEM images of (a) Fe_3O_4 nanoparticles and (b) Fe_3O_4@PDA core−shell nanoparticles.

Polydopamine contains catechol functional groups. Such functional groups can form reversible pH-sensitive boronic acid-catechol conjugates.[18] Recently, the controlled release of a boronic acid analogue anticancer drug bortezomib (BTZ) from a catechol-containing pol(ethylene glycol) was demonstrated.[19] In a neutral or alkaline pH environment, stable boronate esters were formed while in a low pH environment, the group dissociated to release the BTZ drug molecule.[19] Here, we demonstrate a novel use of PDA for controlled drug release using the Fe_3O_4@PDA platform. To investigate the pH-responsive controlled drug release behavior of Fe_3O_4@PDA, BTZ molecules were loaded by soaking Fe_3O_4@PDA into a DMSO solution of BTZ for 24 h. The final adsorption uptake was determined to be ∼34 μmol/g, with ∼34% loading efficiency and 1.44×10^{-12} μmol drug/NP. Supporting Information, Figure S3 demonstrates that the drug-loaded nanoparticles remain a core−shell structure. Figure 2a provides a schematic illustrating that drug molecules are bound to the surface of Fe_3O_4@PDA through reversible covalent bonding according to the reported catechol chemistry.[19]

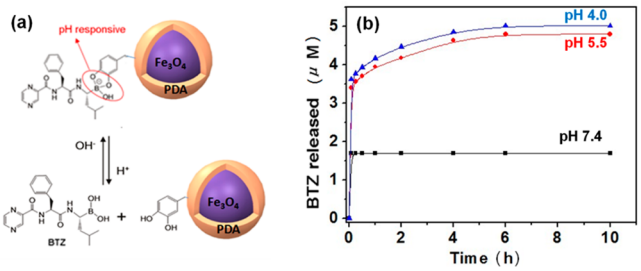

Figure 2. (a) Schematic of pH-dependent boronic acid−catechol conjugates on hybrid core−shell nanoparticle. (b) Time-dependent release of BTZ from Fe_3O_4@PDA core−shell nanoparticles as a function of solution pH ranging from 4−7.4.

The BTZ loaded nanoparticles were dispersed in buffer solutions at different pH values to examine their controlled release property. As illustrated in Figure 2b, the release of BTZ from the nanoparticle surface was pH dependent. At pH 7.4, the release of BTZ occurred within 5 min and saturated at a final concentration of 1.7 μM. At lower pH values, a more gradual release of BTZ was observed. In addition, the final concentration of BTZ in the buffer solution was pH dependent, with a greater concentration observed at lower pH values. The release profiles of BTZ from the Fe_3O_4@PDA NPs are similar to profiles observed from poly(ethylene glycol).[19] However, the current system aims to improve efficacy and reduce toxicity, as NPs can be used to target a specific location. Furthermore, the facile preparation strategy and magnetic operation presents additional advantages of Fe_3O_4@PDA NPs as platform for drug delivery.

Application of Fe_3O_4@PDA core−shell NPs as a catalyst support is demonstrated by directly depositing Au NPs onto Fe_3O_4@PDA core−shell NPs. Au NPs were reduced and grown onto the surface of Fe_3O_4@PDA by facile means of stirring a mixture of Fe_3O_4@PDA and chloroauric acid at 90 °C for 30 min. In this process, the polydopamine shell layer served as both the reducing and the capping agent. The deposition of ∼15 nm diameter Au NPs on the surface of Fe_3O_4@PDA was visually confirmed by TEM (see Figure 3a). The gold-catalyzed reduction of *o*-nitrophenol by $NaBH_4$ to *o*-aminophenol was chosen as a model reaction to evaluate the catalytic capability of the synthesized Au/Fe_3O_4@PDA hybrid NPs (see Figure 3b). The reduction reaction did not proceed without the presence of Au/Fe_3O_4@PDA catalyst, as evidenced by a constant absorption peak at 400 nm (see Supporting Information, Figure S4). However, when Au/Fe_3O_4@PDA catalyst was introduced into the solution, the absorption at 400 nm quickly decreased while the absorption at 295 nm increased (see Figure 3c). The reduction of *o*-nitrophenol into *o*-aminophenol was completed in ∼1 min. The complete conversion of *o*-nitrophenol could also be visually appreciated by the color change of the solution from yellow to clear (see Figure 3b). Stability against coalescence is a very important issue for

dx.doi.org/10.1021/am402585y | ACS Appl. Mater. Interfaces 2013, 5, 9167−9171

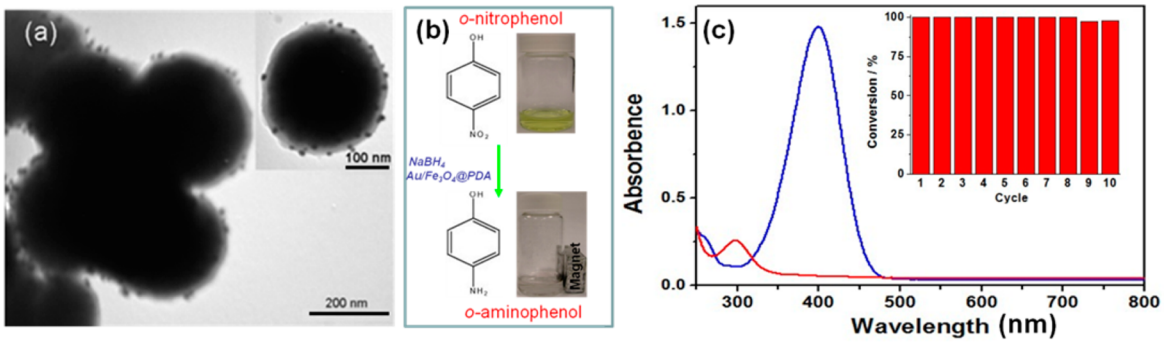

Figure 3. (a) TEM images of Au/Fe_3O_4@PDA hybrid nanoparticles, (b) reaction scheme and illustration of reaction color change, and (c) UV/Vis spectra of *o*-nitrophenol reduction before (blue) and 1 min (red) after the addition of Au/Fe_3O_4@PDA catalyst. Inset: graphic illustration of the conversion of *o*-nitrophenol in 1 min versus the number of catalyst cycles.

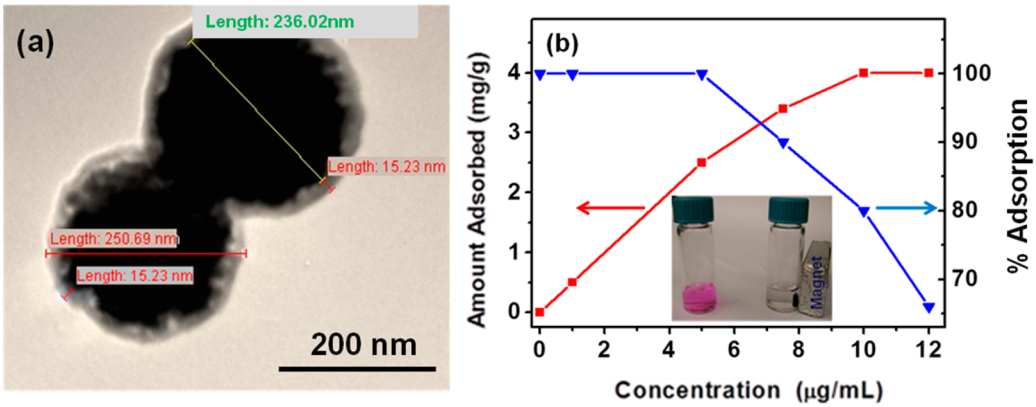

Figure 4. (a) TEM image of Fe_3O_4@C and (b) adsorption isotherm of Rhodamine B on Fe_3O_4@C as a function of concentration at equilibrium. Inset: A digital graph shows an aqueous solution of Rhodamine B (0.005 mg/mL, left) and separation of dye loaded Fe_3O_4@C by a magnet in an identical Rhodamine B solution (right).

nanocrystal-based catalysts.[21−23] The stability of Au/Fe_3O_4@PDA was investigated by repeating the reduction reaction with the same catalyst 10 times (see inset Figure 3c). After each reaction, the catalyst was recycled by magnetic separation, followed by washing with distilled water and drying in vacuum overnight at room temperature. The catalyst showed high activity after 10 successive cycles of reactions, with conversion close to 100% within ∼1 min of reaction time. Au NPs were still clearly visualized on the surface of Fe_3O_4@PDA after 10 reaction cycles (see TEM images in Supporting Information, Figure S5). Clearly, the presence of the PDA shell was efficient in working as a capping agent to stabilize the nanoparticles by preventing their aggregation. Although recyclability is usually regarded as an advantage of nanoparticle-based heterogeneous catalysts, their practical applications in liquid-phase reactions still suffer from both low efficiency of separation and reduced catalytic activity resulting from nanoparticle coagulation.[24] The Au/Fe_3O_4@PDA described here was designed to overcome these challenges. The catalyst can be recovered efficiently from the reaction solution by using external magnetic fields for many cycles without significant losses. Concurrently, the PDA layer effectively stabilizes the catalyst nanoparticles and prevents the reduction in activity due to coagulation, making the catalyst reusable after multiple cycles of reactions. The green synthesis, without the addition of any toxic reducing agents, stability, and recyclability of Au/Fe_3O_4@PDA makes it an attractive platform for nanocatalyst.

Magnetically separable carbon materials are highly attractive for the adsorption and enrichment of organic pollutants associated with liquid-phase processes.[25,26] Among various carbon precursors, polydopamine can be converted to carbon under heat treatment with high carbon yield.[13] We transformed Fe_3O_4@PDA core−shell NPs into Fe_3O_4@C core−shell NPs by pyrolysis in N_2 atmosphere at 600 °C for 1 h. As illustrated in Figure 4a and statistically comparing Fe_3O_4@C to Fe_3O_4@PDA in Figure 1b, the individual Fe_3O_4 core diameters remained unchanged after carbonization, and the carbon shells were uniform and have a thickness of ∼15 nm. The 25% shrinkage of the dopamine shell after carbonization is comparable with the reported 19% shrinkage of another common carbon precursor, resorcinol formaldehyde resin polymer.[27] XRD patterns of Fe_3O_4@C (see Supporting Information, Figure S2) show the same diffraction peaks as Fe_3O_4 nanoparticles. We illustrate the utilization of Fe_3O_4@C as an adsorbent by demonstrating the removal of Rhodamine B from an aqueous solution. As shown in Figure 4b inset, after the addition of Fe_3O_4@C, the Rhodamine B solution (50 μm/mL) color changed within minutes from red to colorless, indicating a quick uptake of Rhodamine B by Fe_3O_4@C. The dye loaded Fe_3O_4@C could be easily separated from the solution by an external magnet. The adsorption was 100% below the initial concentration of 0.005 mg/mL, and the final adsorption capacity of Rhodamine B on Fe_3O_4@C was determined to be 4 mg/g (see Figure 4b). It should be noted that the adsorption capacity of dye on carbon materials is dependent on the

structural properties, pH, and temperature[28,29] and is beyond the focus of the current study.

4. CONCLUSION

In summary, we have developed a facile method to prepare Fe_3O_4@PDA core−shell nanoparticles for multipurpose utilization. The study demonstrated that Fe_3O_4@PDA can be used to control the release of the anti-cancer drug bortezomib by a pH-sensitive manner. The deposition of Au NPs atop Fe_3O_4@PDA can be accomplished through a simple and green method, and the resulting hybrid NPs exhibited high catalytic performance and good reusability for the reduction of *o*-nitrophenol. Fe_3O_4@C was obtained by directly carbonizing Fe_3O_4@PDA and showed a fast adsorption rate and a high adsorption capacity for Rhodamine B removal. The strategy presented in this work provides a facile and versatile approach towards designing Fe_3O_4-based hybrid nanoparticles for biological, energy, and environmental applications.

■ ASSOCIATED CONTENT

Supporting Information

DLS data of Fe_3O_4, XRD patterns of Fe_3O_4 and Fe_3O_4@C, TEM of drug loaded nanoparticles and reused nanocatalyst, and UV-Vis spectra of blank reaction. This material is available free of charge via the Internet at http://pubs.acs.org.

■ AUTHOR INFORMATION

Corresponding Author

*E-mail: rpriestl@princeton.edu.

Notes

The authors declare no competing financial interest.

■ ACKNOWLEDGMENTS

We acknowledge support of the National Science Foundation (NSF) Materials Research Science and Engineering Center program through the Princeton Center for Complex Materials (DMR-0819860) and usage of the PRISM Imaging and Analysis Center at Princeton University.

■ REFERENCES

(1) Liu, J.; Qiao, S. Z.; Hu, Q. H.; Lu, G. Q. *Small* **2011**, *7*, 425−443.
(2) Polshettiwar, V.; Luque, R.; Fihri, A.; Zhu, H. B.; Bouhrara, M.; Basset, J. M. *Chem. Rev.* **2011**, *111*, 3036−3075.
(3) Lu, A. H.; Salabas, E. L.; Schuth, F. *Angew. Chem., Int. Ed.* **2007**, *46*, 1222−1244.
(4) Lee, H.; Dellatore, S. M.; Miller, W. M.; Messersmith, P. B. *Science* **2007**, *318*, 426−430.
(5) Cho, J. H.; Shanmuganathan, K.; Ellison, C. J. *ACS Appl. Mater. Interfaces* **2013**, *5*, 3794−3802.
(6) Liu, N.; Wu, H.; McDowell, M. T.; Yao, Y.; Wang, C. M.; Cui, Y. *Nano Lett.* **2012**, *12*, 3315−3321.
(7) Zhang, M.; Zhang, X.; He, X.; Chen, L.; Zhang, Y. *Nanoscale* **2012**, *4*, 3141−3147.
(8) Ma, Y.; Zhang, X.; Zeng, T.; Cao, D.; Zhou, Z.; Li, W.; Niu, H.; Cai, Y. *ACS Appl. Mater. Interfaces* **2013**, *5*, 1024−1030.
(9) Wang, Y.; Wang, S.; Niu, H.; Ma, Y.; Zeng, T.; Cai, Y.; Meng, Z. *J. Chromatogr. A.* **2013**, *1283*, 20−26.
(10) Lui, K.; Wei, W. Z.; Zeng, J. X.; Liu, X. Y.; Gao, Y. P. *Anal. Bioanal. Chem.* **2006**, *385*, 724−729.
(11) He, H.; Xie, Q.; Yao, S. *J. Colloid Interface Sci.* **2005**, *289*, 446−454.
(12) Ryu, J.; Ku, S. H.; Lee, H.; Park, C. B. *Adv. Funct. Mater.* **2010**, *20*, 2132−2139.
(13) Bernsmann, F.; Richert, L.; Senger, B.; Lavalle, P.; Voegel, J. C.; Schaaf, P.; Ball, V. *Soft Matter* **2008**, *4*, 1621−1624.
(14) Lee, Y.; Lee, H.; Kim, Y. B.; Kim, J.; Hyeon, T.; Park, H. W.; Messersmith, P. B.; Park, T. G. *Adv. Mater.* **2008**, *20*, 4154−4157.
(15) Mrówczyński, R.; Turcu, R.; Leostean, C.; Scheidt, H. A.; Liebscher, J. *Mater. Chem. Phys.* **2013**, *138*, 295−302.
(16) Guo, L.; Liu, Q.; Li, G.; Shi, J.; Liu, J.; Wang, T.; Jiang, G. *Nanoscale* **2012**, *4*, 5864−5867.
(17) Liu, R.; Mahurin, S. M.; Li, C.; Unocic, R. R.; Idrobo, J. C.; Gao, H.; Pennycook, S. J.; Dai, S. *Angew. Chem., Int. Ed.* **2011**, *50*, 6799−6802.
(18) Rowan, S.J.; Cantrill, S.J.; Cousins, G.R.L.; Sanders, J.K.M.; Stoddart, J.F. *Angew. Chem., Int. Ed.* **2002**, *41*, 898−952.
(19) Su, J.; Chen, F.; Cryns, V. L.; Messersmith, P. B. *J. Am. Chem. Soc.* **2011**, *133*, 11850−11853.
(20) Liu, J.; Sun, Z.; Deng, Y.; Zou, Y.; Li, C.; Guo, X.; Xiong, L.; Gao, Y.; Li, F.; Zhao, D. *Angew. Chem., Int. Ed.* **2009**, *48*, 5875−5879.
(21) Arnal, P. M.; Comotti, M.; Schüth, F. *Angew. Chem., Int. Ed.* **2006**, *45*, 8224−8227.
(22) Comotti, M.; Pina, C. D.; Matarrese, R.; Rossi, M. *Angew. Chem., Int. Ed.* **2004**, *43*, 5812−5815.
(23) Valdés-Solís, T.; Valle-Vigón, P.; Sevilla, M.; Fuertes, A. B. *J. Catal.* **2007**, *251*, 239−243.
(24) Ge, J.; Zhang, Q.; Zhang, T.; Yin, Y. *Angew. Chem., Int. Ed.* **2008**, *47*, 8924−8928.
(25) Zhang, Z. Y.; Kong, J. L. *J. Hazard. Mater.* **2011**, *193*, 325−329.
(26) Wang, D. W.; Li, F.; Lu, G. Q.; Cheng, H. M. *Carbon* **2008**, *46*, 1593−1599.
(27) Liu, J.; Qiao, S. Z.; Liu, H.; Chen, J.; Orpe, A.; Zhao, D.; Lu, G. Q. *Angew. Chem., Int. Ed.* **2011**, *50*, 5947−5951.
(28) Arivoli, S.; Thenkuzhali, M. *E-J. Chem.* **2008**, *5*, 187−200.
(29) Guo, Y. P.; Zhao, J. Z.; Zhang, H.; Yang, S. F.; Qi, J.R.; Wang, Z. C.; Xu, H. D. *Dyes Pigments* **2005**, *66*, 123−128.